DNA “Motors” and Actuators

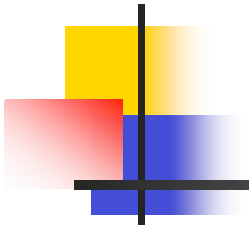

- B-Z Transition. Ionic switching.
- Tweezers/scissors. Annealing.
- G-Tetrad. G-Quartet. Annealing.
- DNA Supercoiling. Ionic switching.
- PX-JX Transition. Annealing.
- Two-state Lattice. Annealing.
- Walkers. Annealing or DNAzyme.

A nanomechanical device based on the B–Z transition of DNA

Chengde Mao, Weiqiong Sun, Zhiyong Shen & Nadrian C. Seeman

Department of Chemistry, New York University, New York, New York 10003, USA

NATURE | VOL 397 | 14 JANUARY 1999

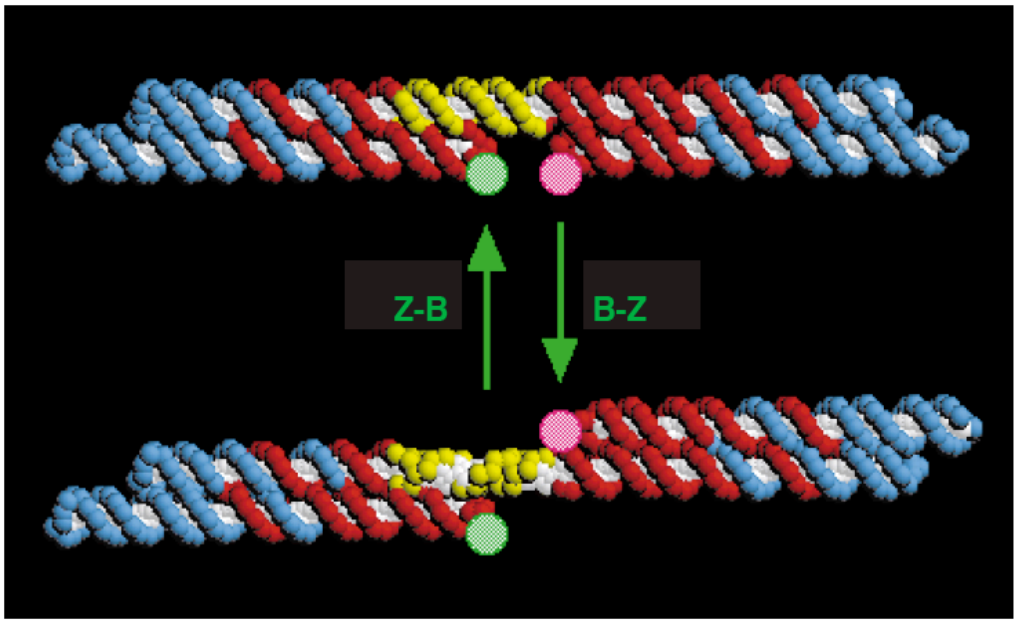

green (fluorescein) and magenta (Cy3)

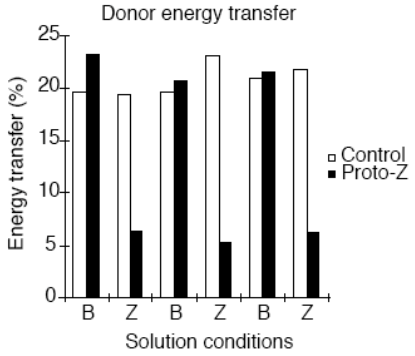

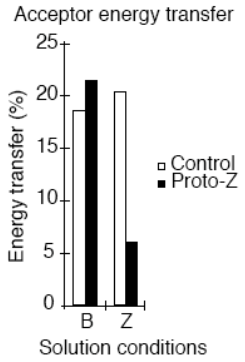

Figure 2 FRET demonstration of nanomechanical motion. Top, energy transfe measured from the decrease in donor fluorescence when cycling the systen alternately through B and Z conditions. A similar result is obtained when the increase in acceptor fluorescence is used (bottom). In both graphs, the molecule containing the proto-Z segment is contrasted with a control that lacks it. Only the molecule containing the proto-Z segment shows a change in energy transfer in Z promoting conditions.

The double helix connecting the two DAO molecules contains the base-paired sequence $d(CG)_{10}$, a 'proto-Z' sequence that can be converted to left-handed Z-DNA at high ionic strength; the 5-position of cytosine is methylated, a modification that increases the propensity of DNA to undergo the B–Z transition[21]; as a result, we are able to promote the transition with a 10 mM cacodylate buffer (pH 7.5) containing 0.25 mM $Co(NH_3)_6Cl_3$, 100 mM $MgCl_2$ and 100 mM NaCl, whereas B-DNA is present when the same buffer contains 10 mM $MgCl_2$, 100 mM NaCl and no $Co(NH_3)_6Cl_3$.

A DNA-fuelled molecular machine made of DNA

Bernard Yurke*, Andrew J. Turberfield*†, Allen P. Mills Jr*, Friedrich C. Simmel* & Jennifer L. Neumann*

** Bell Laboratories, Lucent Technologies, 600 Mountain Avenue, Murray Hill New Jersey 07974, USA*
† Department of Physics, University of Oxford, Clarendon Laboratory, Parks Road, Oxford OX1 3PU, UK

NATURE | VOL 406 | 10 AUGUST 2000 |

Here we report the construction of a DNA machine in which the DNA is used not only as a structural material, but also as 'fuel'. The machine, made from three strands of DNA, has the form of a pair of tweezers. It may be closed and opened by addition of auxiliary strands of 'fuel' DNA; each cycle produces a duplex DNA waste product.

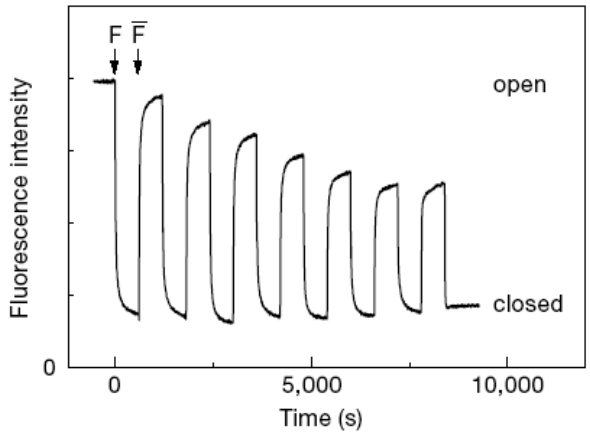

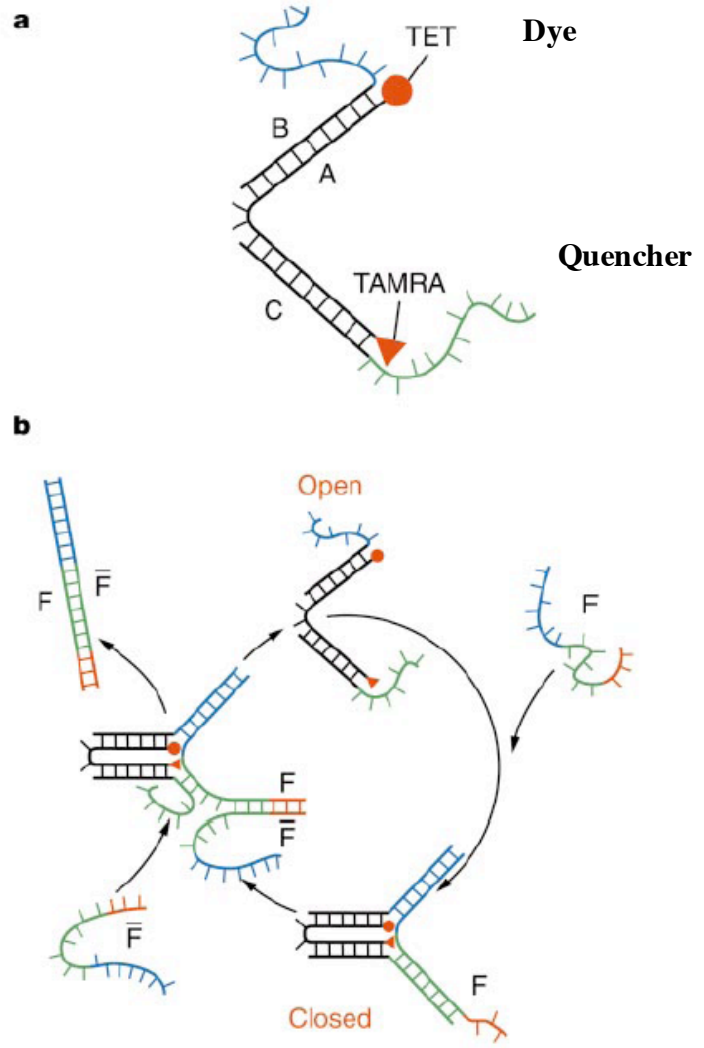

Figure 2 Construction and operation of the molecular tweezers. **a**, Molecular tweezer structure formed by hybridization of oligonucleotide strands A, B and C. **b**, Closing an opening the molecular tweezers. Closing strand F hybridizes with the dangling ends o strands B and C (shown in blue and green) to pull the tweezers closed. Hybridization wi the overhang section of F (red) allows F̄ strand to remove F from the tweezers, forming double-stranded waste product FF̄ and allowing the tweezers to open. Complementar

NATURE | VOL 406 | 10 AUGUST 2000 |

- **Toe-hold binding.**
- **Strand invasion.**
- **Branch diffusion.**

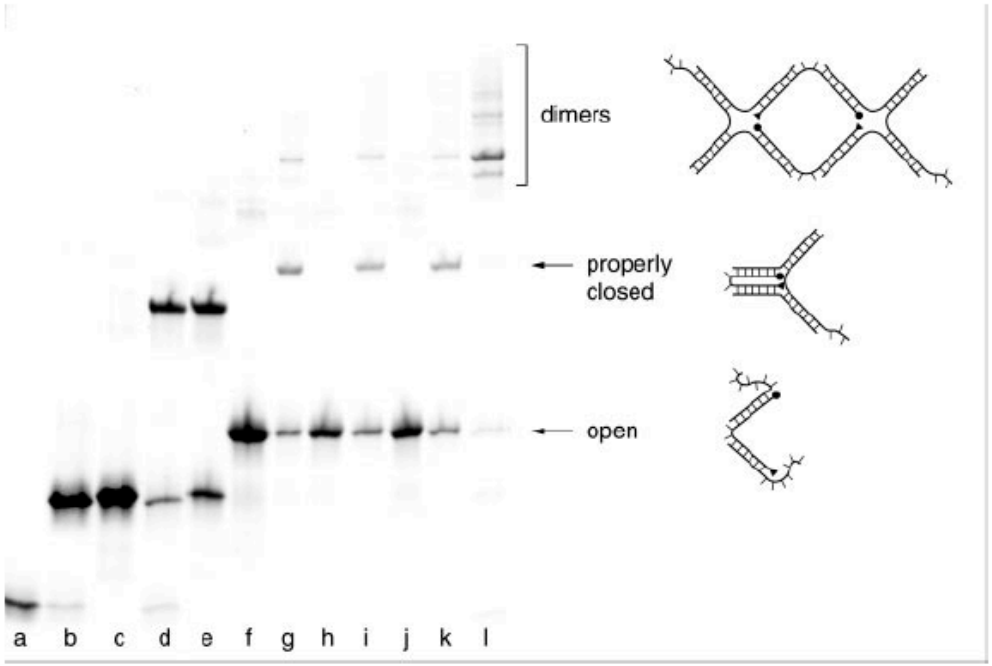

Figure 4 Analysis of tweezer formation by polyacrylamide gel electrophoresis. Lanes as follows: a, strand A; b, A+C; c, A+B; d, A+C+F; e, A+B+F; f, A+B+C (open tweezers); g, (A+B+C)+F (closed tweezers); h–k, two further cycles of opening and closing produced by successive additions of $\bar{F}$ and F to closed tweezers; l, (A,B,C)+(A,β,γ)+$F_{Bγ}$+$F_{Cβ}$ (only dimers can form). Schematic structures of open and properly closed tweezers and of a dimer complex are shown next to the appropriate bands.

PHYSICAL REVIEW E, VOLUME 63, 041913

Using DNA to construct and power a nanoactuator

Friedrich C. Simmel and Bernard Yurke
Bell Laboratories, Lucent Technologies, Murray Hill, New Jersey

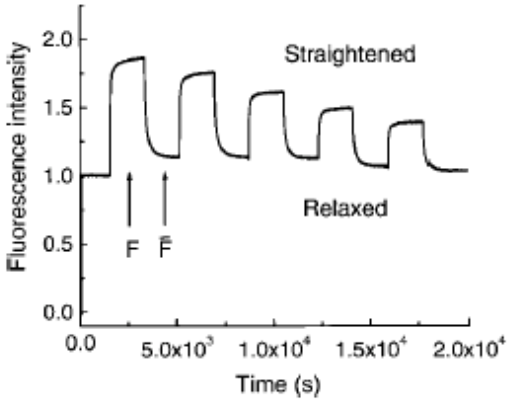

FIG. 2. The fluorescence intensity as a function of time as the actuator is successively straightened and relaxed. When F is added, the fluorescence increases due to the increased distance between the TET and TAMRA dyes. When $\bar{F}$ is added the fluorescence decreases.

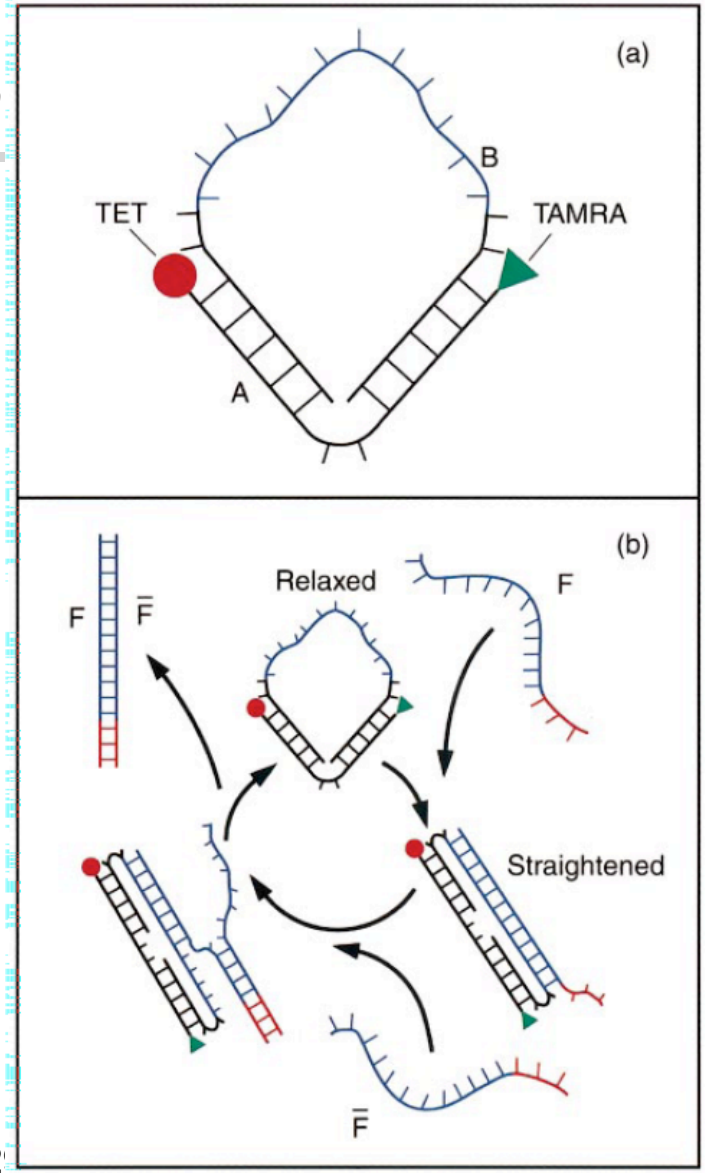

Nucleic Acid Supercoiling as a Means for Ionic Switching of DNA – Nanoparticle Networks

Christof M. Niemeyer,*[a] Michael Adler,[a] Steven Lenhert,[b] Song Gao,[b] Harald Fuchs,[b] and Lifeng Chi[b]

Oligomeric nanoparticle networks, generated by the self-assembly of bis-biotinylated double-stranded DNA fragments and streptavidin, have been studied by scanning force microscopy (SFM). SFM imaging revealed the presence within the networks of irregular thick DNA molecules, which were often associated with distinct, Y-shaped structural elements. Closer analysis revealed that the Y structures are formed by condensation (thickening and shortening) of two DNA fragments, most likely through the supercoiling of two DNA molecules bound to adjacent binding sites of the streptavidin particle. The frequency of supercoiling was found to be dependent on the ionic strength applied during the immobilization of the oligomeric networks on mica surfaces. Potential applications of the structural changes as a means for constructing ion-dependent molecular switches in nanomaterials are discussed.

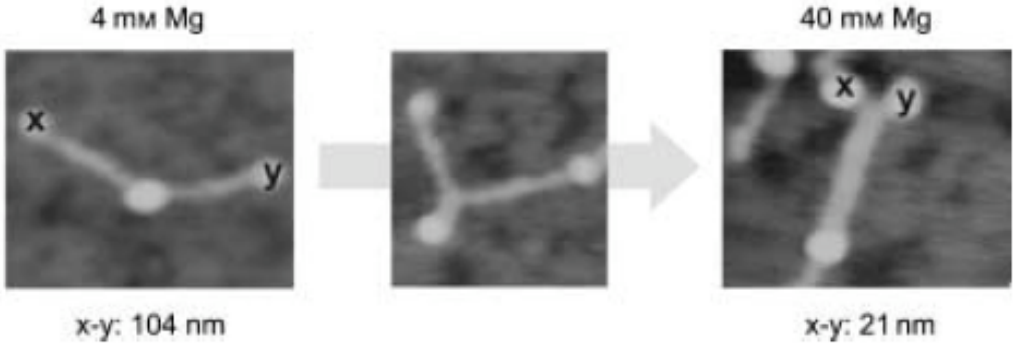

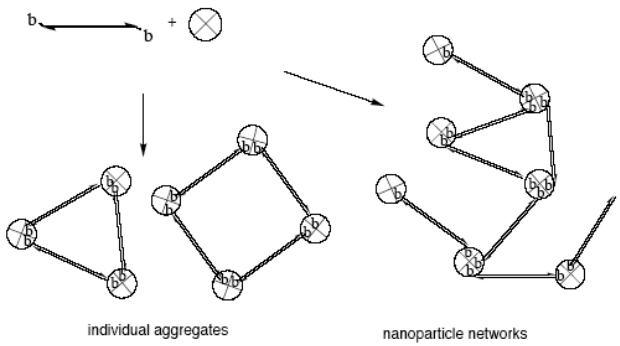

C. M. Niemeyer, M. Adler, S. Lenhert, S. Gao, H. Fuchs, L. F. Chi, *ChemBioChem* **2001**, *2*, 260–265.

C. M. Niemeyer, M. Adler, S. Lenhert, S. Gao, H. Fuchs, L. F. Chi, *ChemBioChem* **2001**, *2*, 260–265.

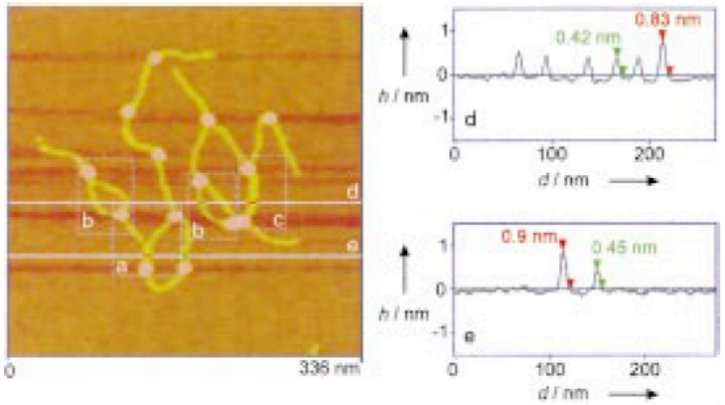

Figure 2. *Scanning force microscopy analysis of a typical oligomeric network obtained from the assembly of STV and bis-biotinylated 169 base-pair dsDNA fragments. Individual structure elements are indicated: a) symmetric Y-type structure; b) binary assembly linked by two regular DNA fragments; c) binary assembly linked by a supercoil of two DNA fragments; d) cross-section through regular and supercoiled DNA; e) cross-section through regular and partially supercoiled DNA. Height measurements* h *along the lines (d) and (e) are shown on the right. Note that the supercoiled DNA has about twice the height of the regular DNA.*

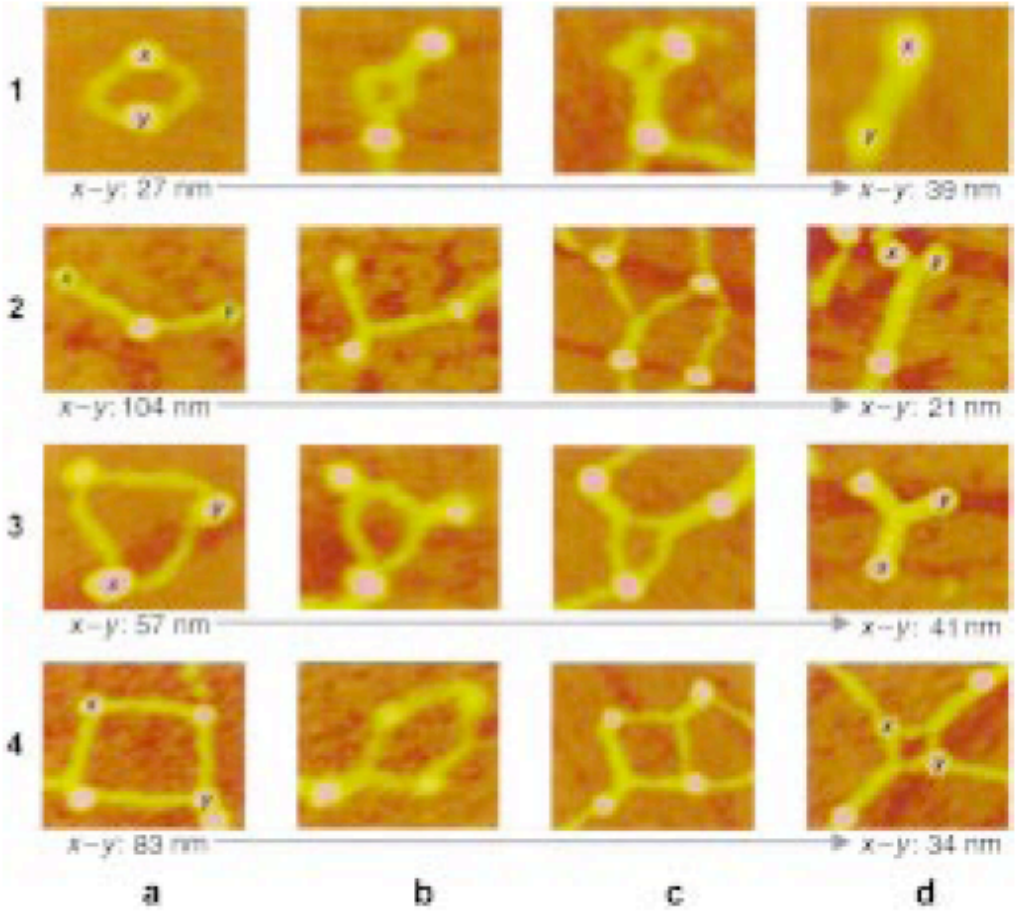

Figure 4. *Ionic switching of nanoparticle networks. The relative orientation of the STV particles is altered by increased condensation of the interconnecting DNA linkers. The SFM images indicate structural changes observed in representative DNA_2-STV_2 (**1**), DNA_2-STV_3 (**2**), DNA_3-STV_3 (**3**), and DNA_4-STV_4 (**4**) elements that occur in the random oligomeric networks. Note that the structures of type **a** represent the extended species, while types **b** and **c** are assigned as intermediates during the formation of type **d**, the species that contains fully condensed DNA fragments.*

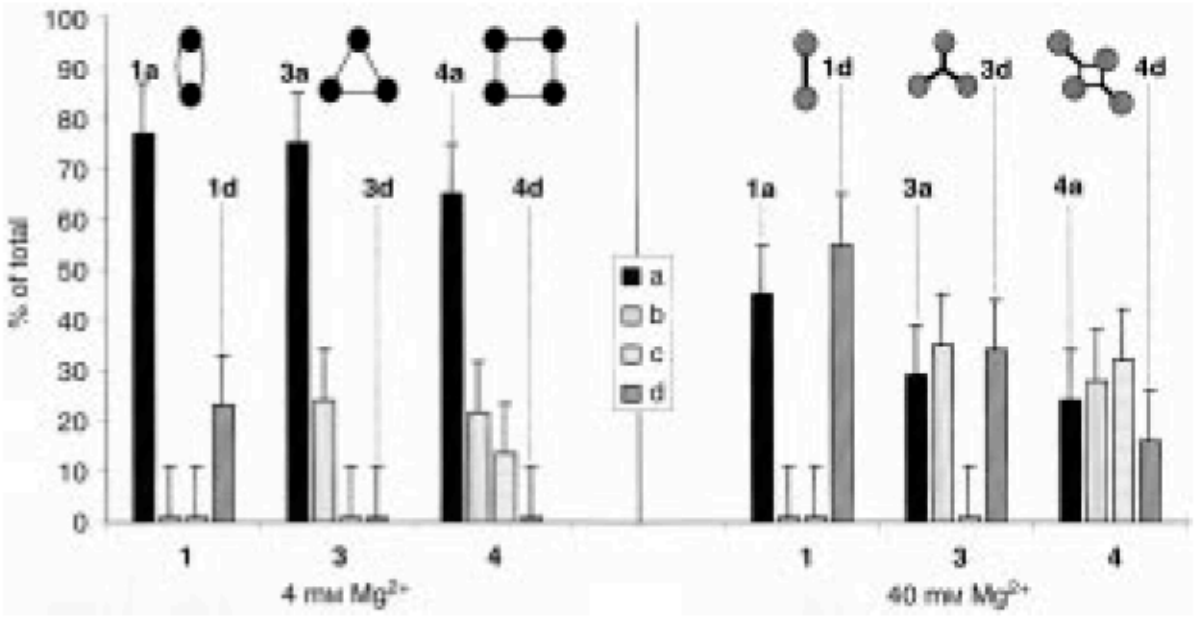

Figure 5. *Statistical evaluation of the ion-dependent relative abundance of the structural intermediates* ***a*** *–* ***d*** *(Figure 4). The heights of the histograms represent the percentage of the individual species according to the concentration of $MgCl_2$ used for immobilization. The total number of dsDNA molecules counted was greater than 1500. Note the increased abundance of the condensed species at 40 mM $MgCl_2$. The intermediates* ***b*** *and* ***c*** *are scarce for the dimer* ***1****, while in the case of the trimer* ***3*** *and tetramer* ***4****, the intermediates* ***b*** *and* ***c****, which contain symmetrical Y-type DNA structures, are present to a greater extent.*

C. M. Niemeyer, M. Adler, S. Lenhert, S. Gao, H. Fuchs, L. F. Chi,
ChemBioChem **2001**, *2*, 260–265.

A Single DNA Molecule Nanomotor

Jianwei J. Li and Weihong Tan*

Center for Research at the Bio-nano Interface, Department of Chemistry and the McKnight Brain Institute, University of Florida, Gainesville, Florida 32611

NANO LETTERS

2002
Vol. 2, No. 4
315−318

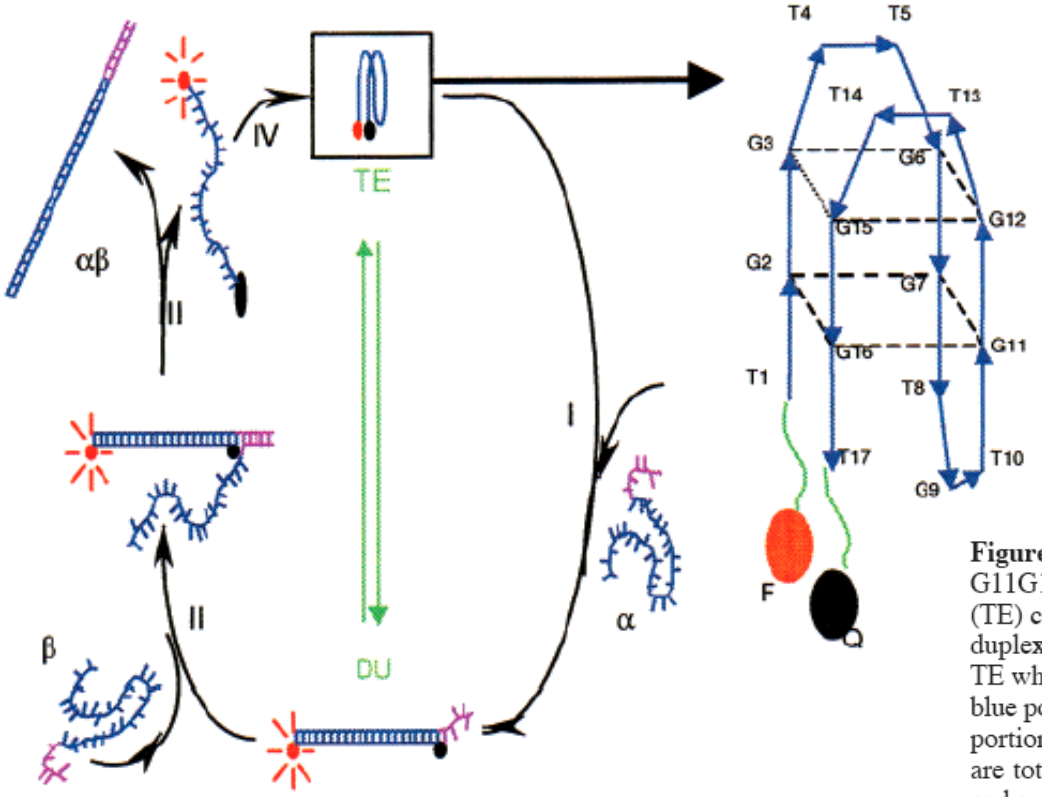

5' TGGTTGGTGTGGTTGGT 3'

Figure 1. 17mer DNA nanomotor (T1G2G3T4T5G6G7T8G9T10 G11G12T13T14G15G16T17) can adopt an intramolecular tetraplex (TE) conformation, as indicated by the thick arrow. It extends into duplex (DU) when it hybridizes to strand α and shrinks back to TE when strand α is displaced via hybridization with strand *β*. The blue portion in α is complementary to the nanomotor, and the purple portion represents extra bases to form sticky ends in DU. α and *β* are totally complementary to each other. A fluorophore (red ball) and a quencher (black ball) are connected through two linkers (green lines) to the ends of the 17-mer to report the motion of the nanomotor, which is shown as two layers of G tetrads.[5]

NANO LETTERS

2002
Vol. 2, No. 4
315−318

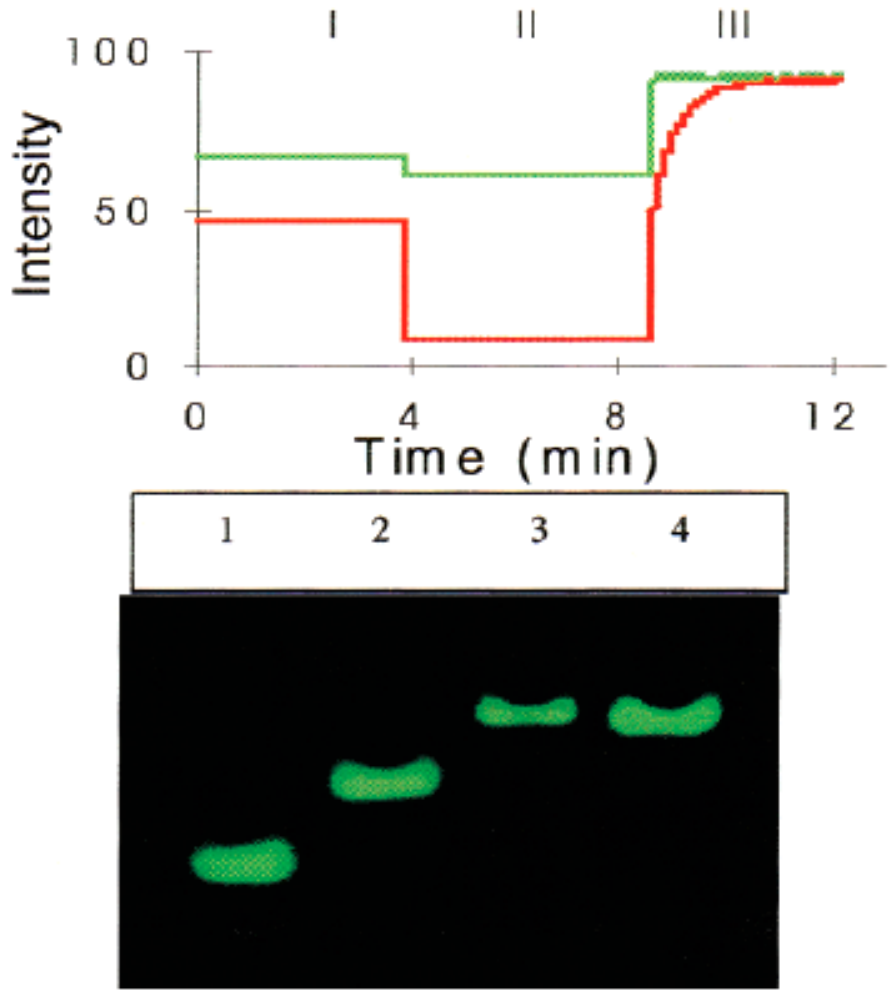

Figure 2. (a) Fluorescent response of the nanomotor 17mer (red) and the S17mer (green) (I) to the addition of K^+ (II) and to the addition of complementary sequences (III): I, no salt; II, added 10 mM K^+; III, added α. (b) Gel electrophoresis: 1, nanomotor; 2, S17mer; 3, nanomotor plus α; 4, S17mer plus its complementary sequence.

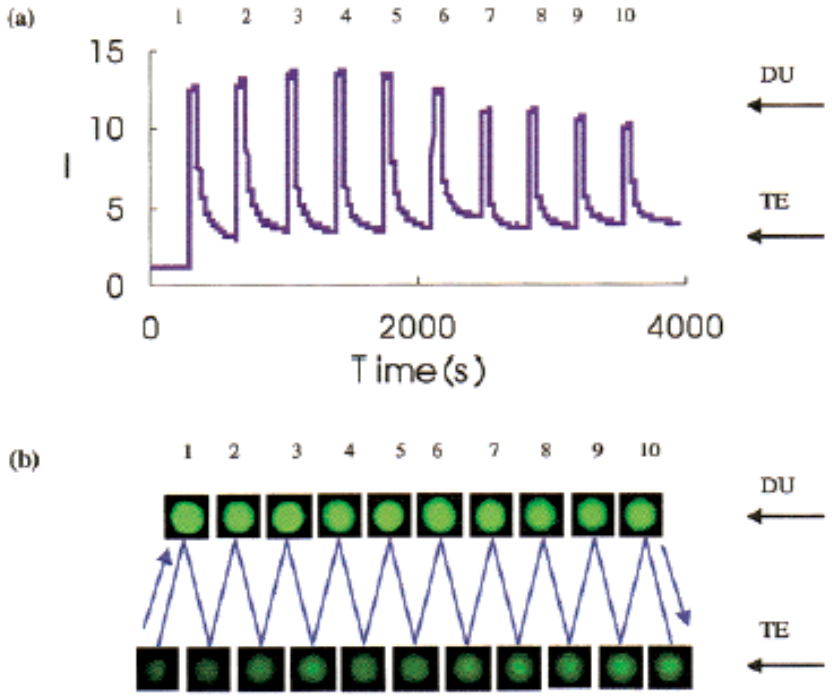

Figure 3. Cycling of the DNA nanomotor. During the nanomotor's cycling, the fluorescence intensity is recorded either by a spectrofluorometer (top) or by a digital camera (bottom). Ten cycles were recorded here.

NANO LETTERS

2002
Vol. 2, No. 4
315−318

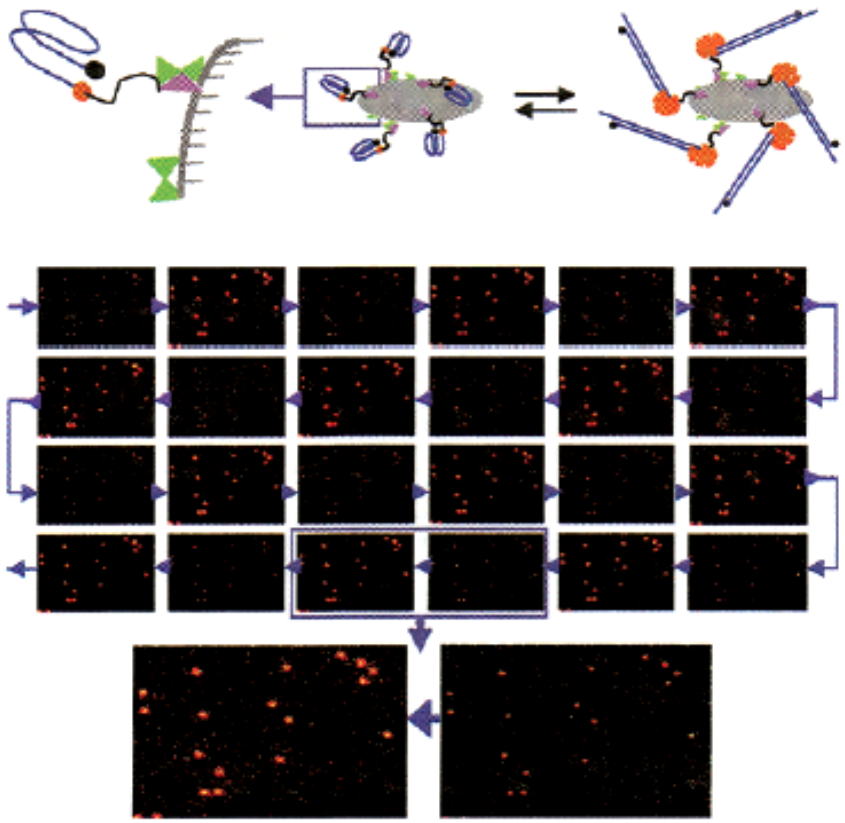

Figure 4. (a) Schematic representation of the triple labeled nanomotor immobilized onto nanoparticles, turning its fluorescence signal on and off upon exposure to strand α/strand β: F, fluorophore; Q, quencher; L, linker; B, biotin; S, streptavidin; N, nanoparticle surface. (b) Images of nanoparticles with nanomotors cycling on the surface. Nanomotor-nanoparticles are immobilized onto the inner surface of a microchannel. Cycling was conducted by flushing α and β solutions alternatively through the microchannel. The arrows indicate the order of recording the images.

We have estimated the ideal energy conversion efficiency, *f*, which is dependent on the length of the sticky end in strand α. For a 10 base long sticky end, *f* is 0.63, while *f* rises to 0.94 when the sticky end is shortened to 1 base. The theoretical extending force, F_{ex}, and shrinking force, F_{sh}, were also estimated. At 37 °C and with 25 mM KCl, F_{ex} and F_{sh} were calculated to be 20.7 and 2.2 pN, respectively. While the shrinking force is close to the forces determined for kinesin and myosin protein motors, the extending force is about 10 times larger than those protein nanomotors.[12] The forces are tunable through changing the solution conditions.

DNA duplex–quadruplex exchange as the basis for a nanomolecular machine

PNAS | February 18, 2003 | vol. 100 | no. 4 | 1569–1573

Patrizia Alberti and Jean-Louis Mergny*

Laboratoire de Biophysique, Muséum National d'Histoire Naturelle, Institut National de la Santé et de la Recherche Médicale Unité 565, Centre National de la Recherche Scientifique Unité Mixte de Recherche 8646, 43 Rue Cuvier, 75005 Paris, France

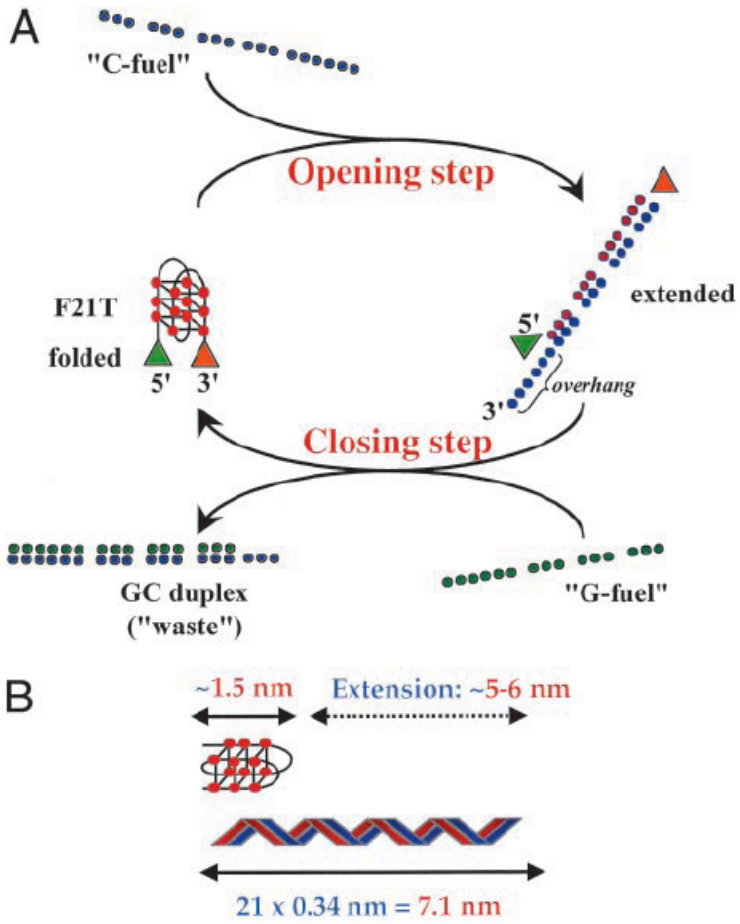


```
                                F-5'-GGGTTAGGGTTAGGGTTAGGG-3'-T   F21T
C-fuel strands:
                          3'-CCCAATCCCAATCCCAATCCC-5'      21C
                    3'-tgcaatCCCAATCCCAATCCCAATCCC-5'      27C
                    3'-tgcaatCCGAATCGCAATCACAATCCC-5'      27Cm3C
               3'-gcctgcaatCCCAATCCCAATCCCAATCCC-5'        30C
3'-atagcctgcaatCCCAATCCCAATCCCAATCCC-5'                   33C

G-fuel strands:
                    5'-acgttaGGGTTAGGGTTAGGGTTA-3'        24G
                    5'-acgttaGGCTTAGCGTTAGTGTTA-3'        24Gm3G
                    5'-ctacctGGGTTAGGGTTAGGGTTA-3'        24Gmut
               5'-cggacgttaGGGTTAGGGTTAGGGTTA-3'          27G
5'-tatcggacgttaGGGTTAGGGTTAGGGTTA-3'                      30G
```

Fig. 2. Sequence of the oligonucleotides used in this study. Names are given on the right side. (*Top*) G-quadruplex forming oligonucleotide. F, fluorescein; T, tetramethylrhodamine. The 3′ overhang (6–12 bases long) present on the C-fuel strands is shown with lowercase letters. Mismatched bases (with respect to the F21T oligonucleotide) are underlined and boldfaced. The 5′ overhang on the G-fuel strand is shown with lowercase letters. For the 24Gmut control oligonucleotide, this overhang is not complementary to the last six bases of the C-fuel strand and is therefore presented with underlined and bold letters.

Compare previous...

5' TGGTTGGTGTGGTTGGT 3'

PNAS | February 18, 2003 | vol. 100 | no. 4 | 1569–1573

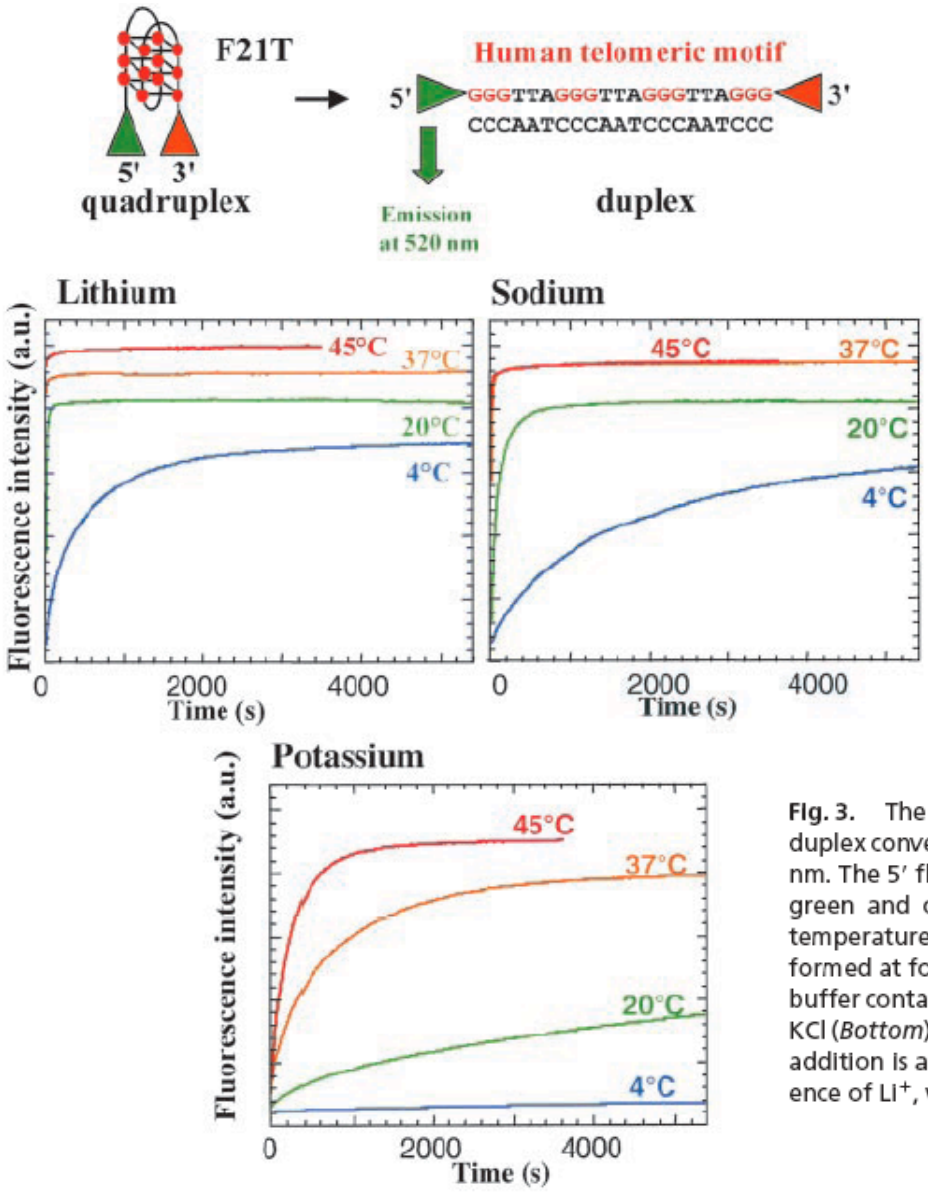

Fig. 3. The opening step. (*Top*) Principle of the experiment. Quadruplex-to-duplex conversion is monitored by an increase in fluorescence emission at 520 nm. The 5′ fluorescein and 3′ tetramethylrhodamine groups are depicted by green and orange triangles, respectively. (*Middle* and *Bottom*) Effect of temperature on quadruplex-to-duplex conversion. All experiments were performed at four different temperatures in a 10 mM sodium cacodylate pH 7.2 buffer containing 0.1 M LiCl (*Middle Left*), 0.1 M NaCl (*Middle Right*), or 0.1 M KCl (*Bottom*). The predominant starting structure ($t = 0$ s) before C-fuel strand addition is always an intramolecular quadruplex, except at 45°C in the presence of Li^+, where F21T is mainly single-stranded.

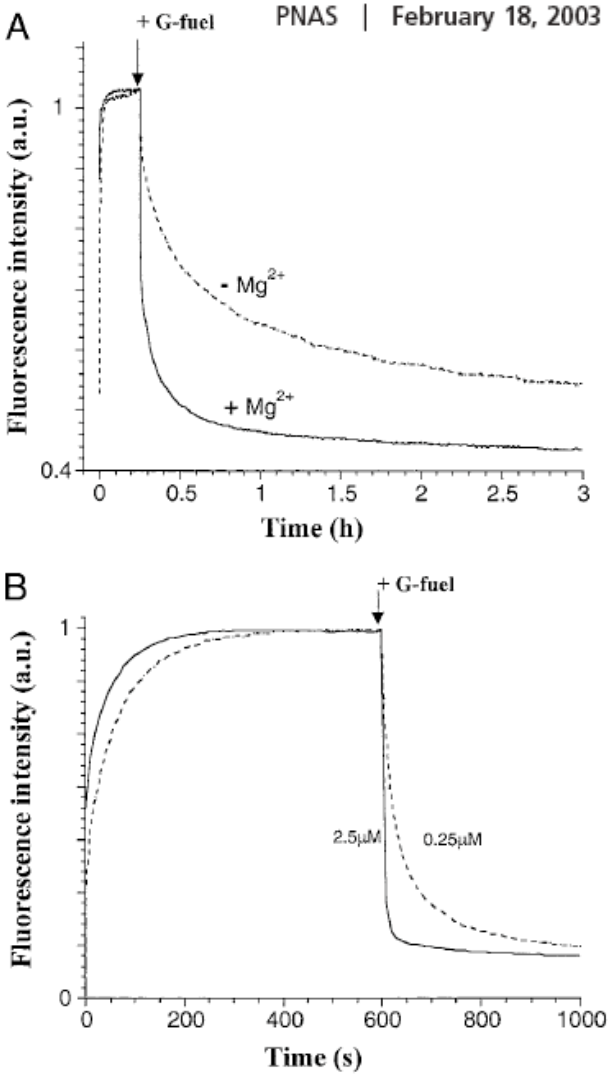

Fig. 4. Optimization of the device. (*A*) Effect of magnesium. Only one cycle is presented. The closing step is much faster in the presence (solid line) than in the absence (dashed line) of 20 mM $MgCl_2$. The experiment was performed at 37°C in a 100 mM NaCl/10 mM sodium cacodylate (pH 7.2) buffer. F21T, 33C, and 30G oligonucleotide concentrations were 0.2, 0.25, and 0.25 μM, respectively. (*B*) Concentration dependency. All experiments were performed at 45°C in a 20 mM $MgCl_2$/100 mM KCl/10 mM sodium cacodylate (pH 7.2) buffer. On the dotted line, the concentrations for F21T, C-fuel (3′-TGCAATGCCAATCGCAATCGCAATCCC-5′ 27Cm3C), and G-fuel (5′-ACGTTACGGTTAGCGTTAGCGTTA-3′ 24Gm3G) are 0.2, 0.25, and 0.25 μM, respectively. The full line presents a similar experiment with a 10-fold increase in all oligonucleotide concentrations (normalized fluorescence intensity).

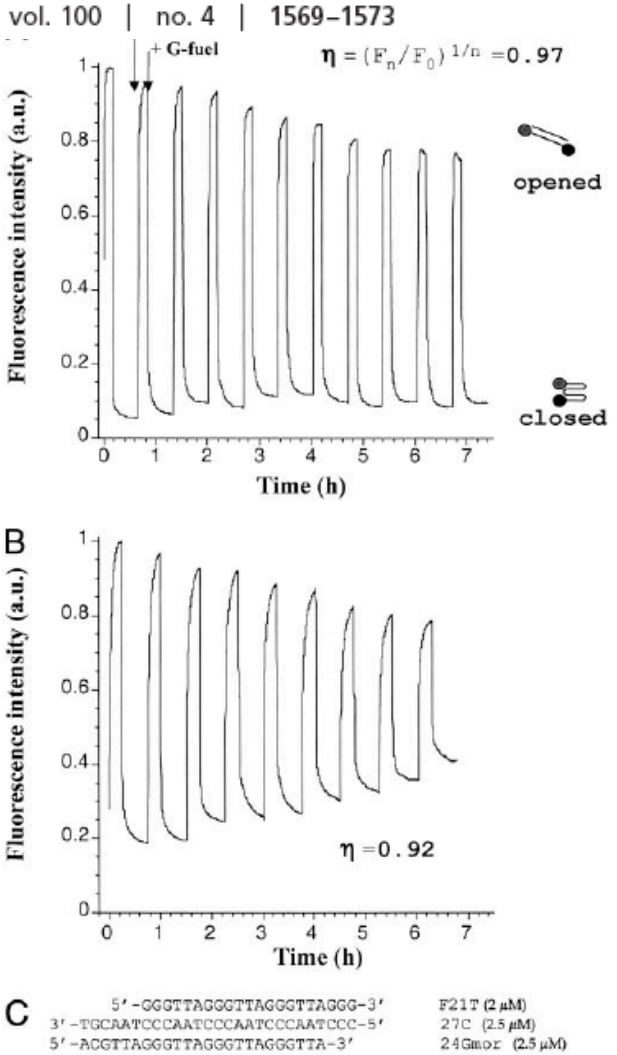

Fig. 5. Cycling the device. (*A*) With DNA strands. By alternatively adding stoichiometric amounts of the C-fuel (27Cm3C; 2.5 μM) and G-fuel (24Gm3G; 2.5 μM) strands, F21T may be opened and closed repeatedly (at least 11 times); for purposes of clarity, the times of C- and G-fuel additions are indicated for only one cycle. Each addition of the C- or G-fuel strand results in a 0.5% dilution of the reactants, which is mathematically corrected on this graph. Experimental conditions: 100 mM KCl/20 mM $MgCl_2$/10 mM sodium cacodylate (pH 7.2) at 45°C. η, the average cycling efficiency (3% loss per cycle). (*B*) Cycling with a modified oligonucleotide. The G-fuel strand is a chemically modified oligonucleotide (morpholino, with a neutral backbone, synthesized by Gene Tools). Nine successive cycles are shown. Despite a careful assessment of strand concentrations, each successive cycle leads to a significant loss in signal. The experiment was performed in a 100 mM KCl/10 mM sodium cacodylate (pH 7.2) buffer at 45°C (no magnesium). Oligonucleotide sequences are shown in *C*.

A robust DNA mechanical device controlled by hybridization topology

NATURE | VOL 415 | 3 JANUARY 2002

Hao Yan, Xiaoping Zhang, Zhiyong Shen & Nadrian C. Seeman

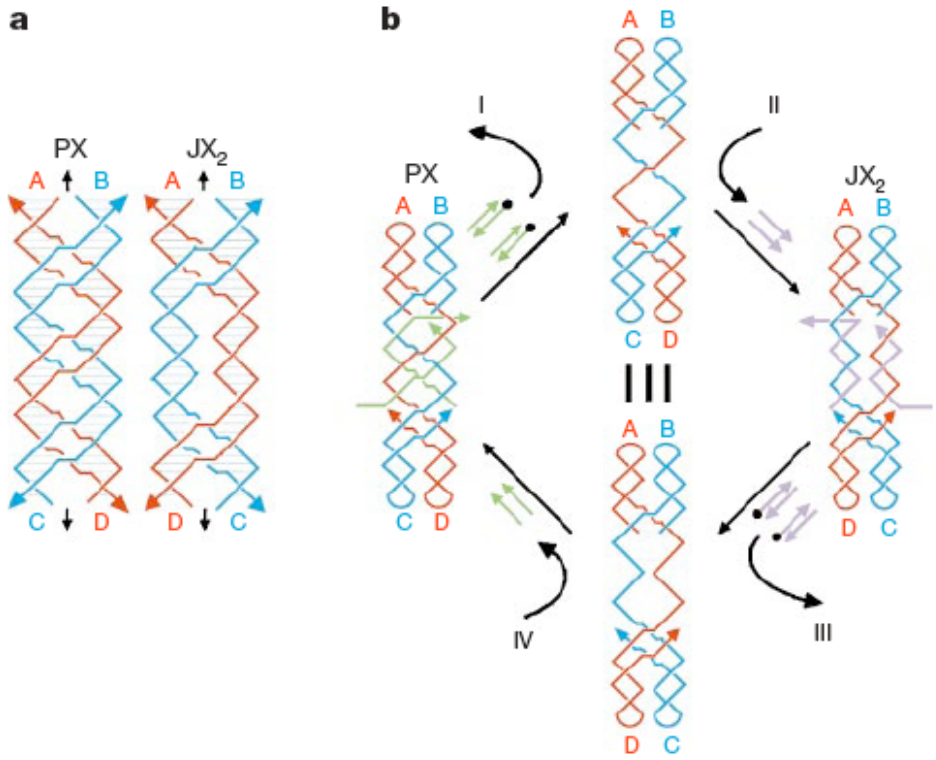

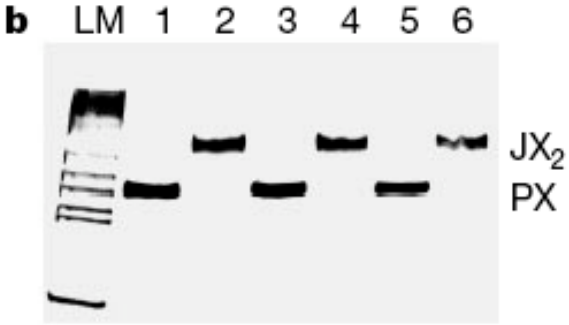

NATURE | VOL 415 | 3 JANUARY 2002

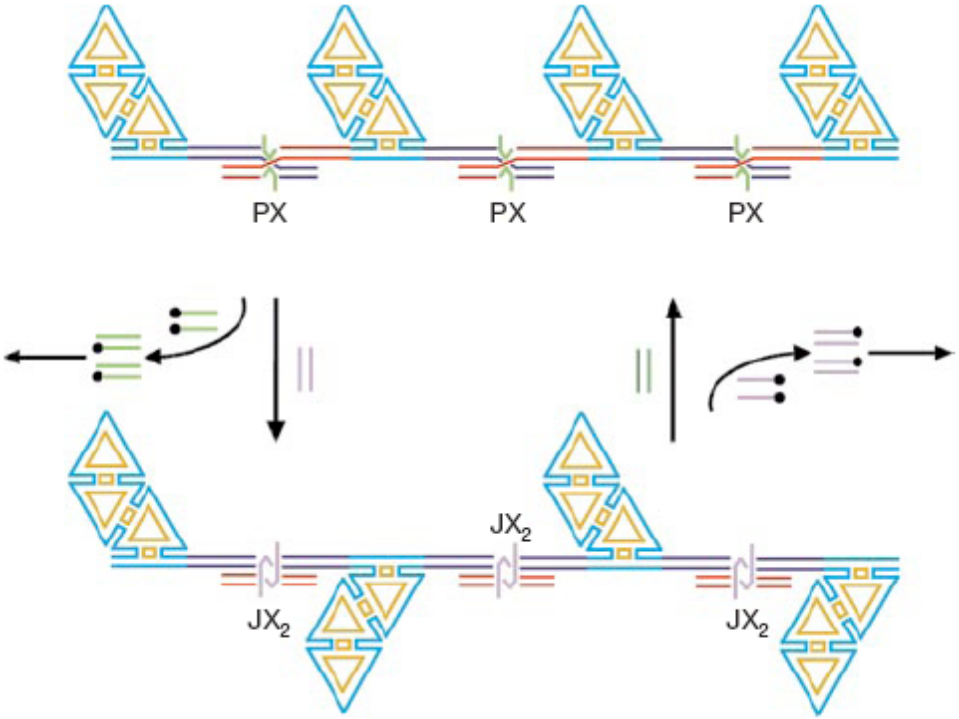

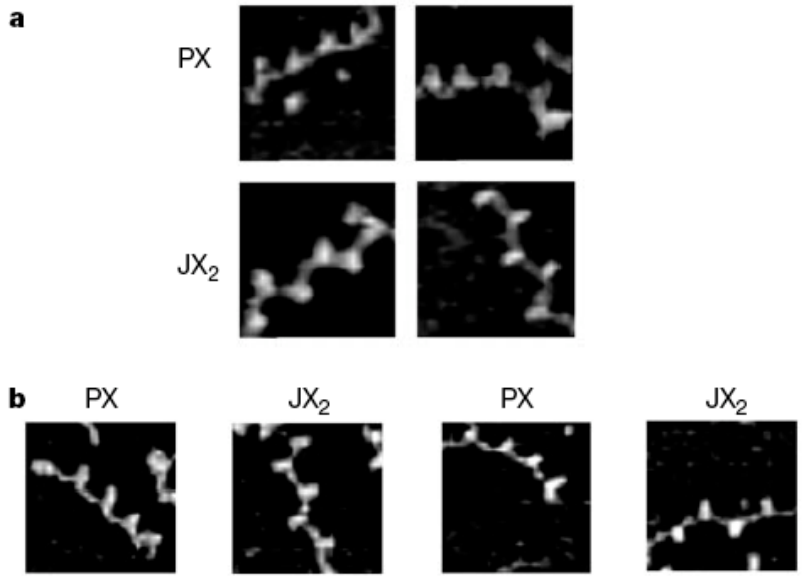

Nanomechanical Device

A Two-State DNA Lattice Switched by DNA Nanoactuator**

*Liping Feng, Sung Ha Park, John H. Reif, and Hao Yan**

Angew. Chem. Int. Ed. **2003**, *42*, 4342–4346

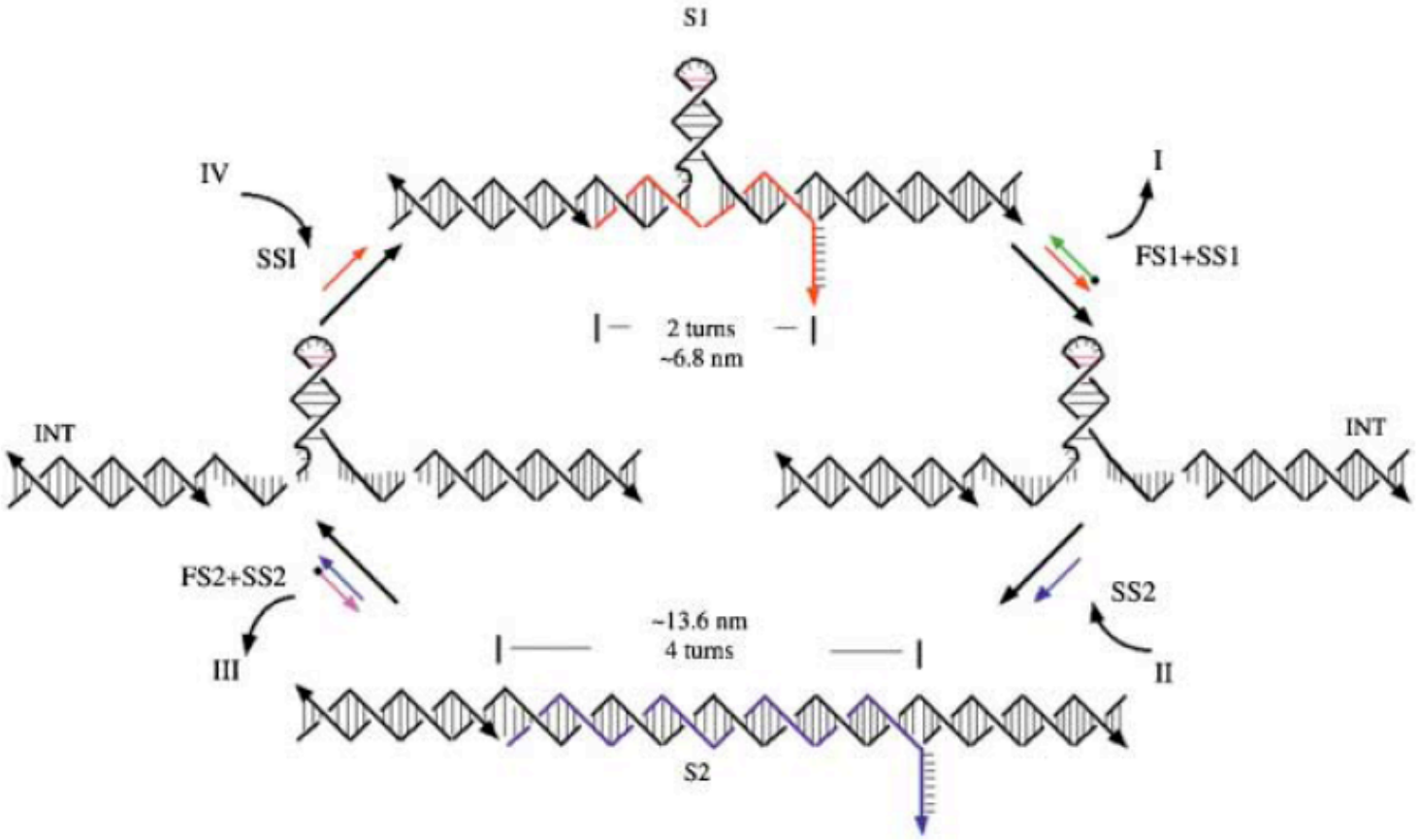

Angew. Chem. Int. Ed. 2003, 42, 4342–4346

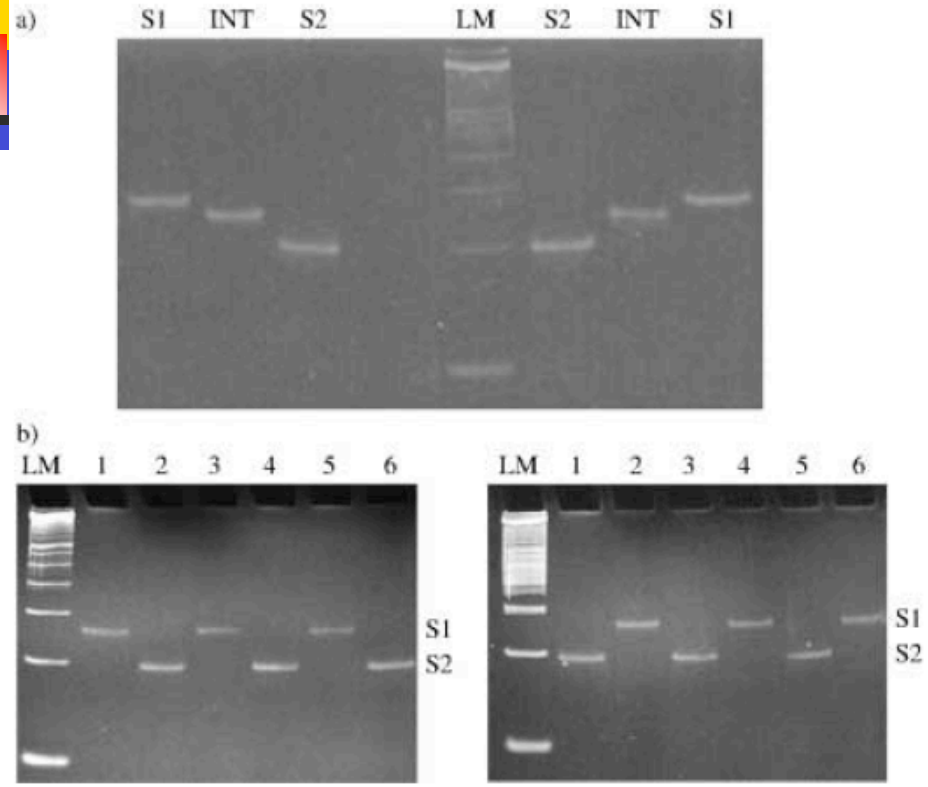

Figure 2. Gel evidence for the cycling of the nanoactuator device. See text for an explanation.

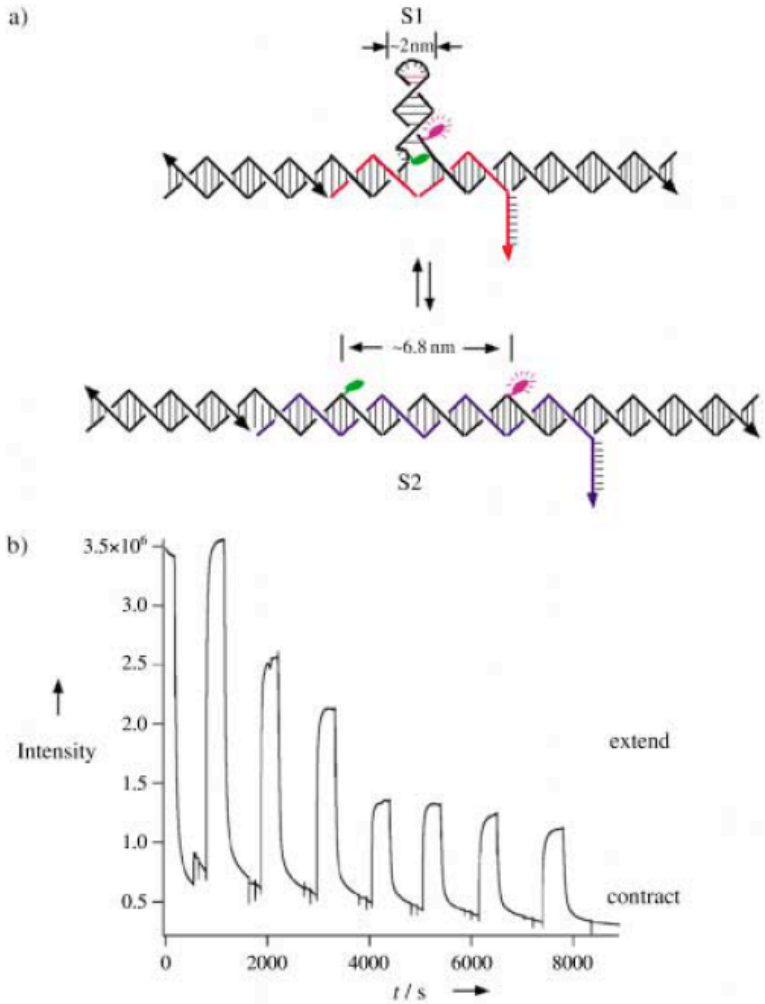

Figure 3. FRET measurements for the cycling of the nanoactuator device. a) Schematic drawing of the incorporation of fluorescent dyes in the nanoactuator device. A donor, fluorescein, and an acceptor, Tamra,are represented as green and purple filled circles, respectively. b) Cycling the nanoactuator device measured by FRET spectroscopy.

Angew. Chem. Int. Ed. 2003, 42, 4342–4346

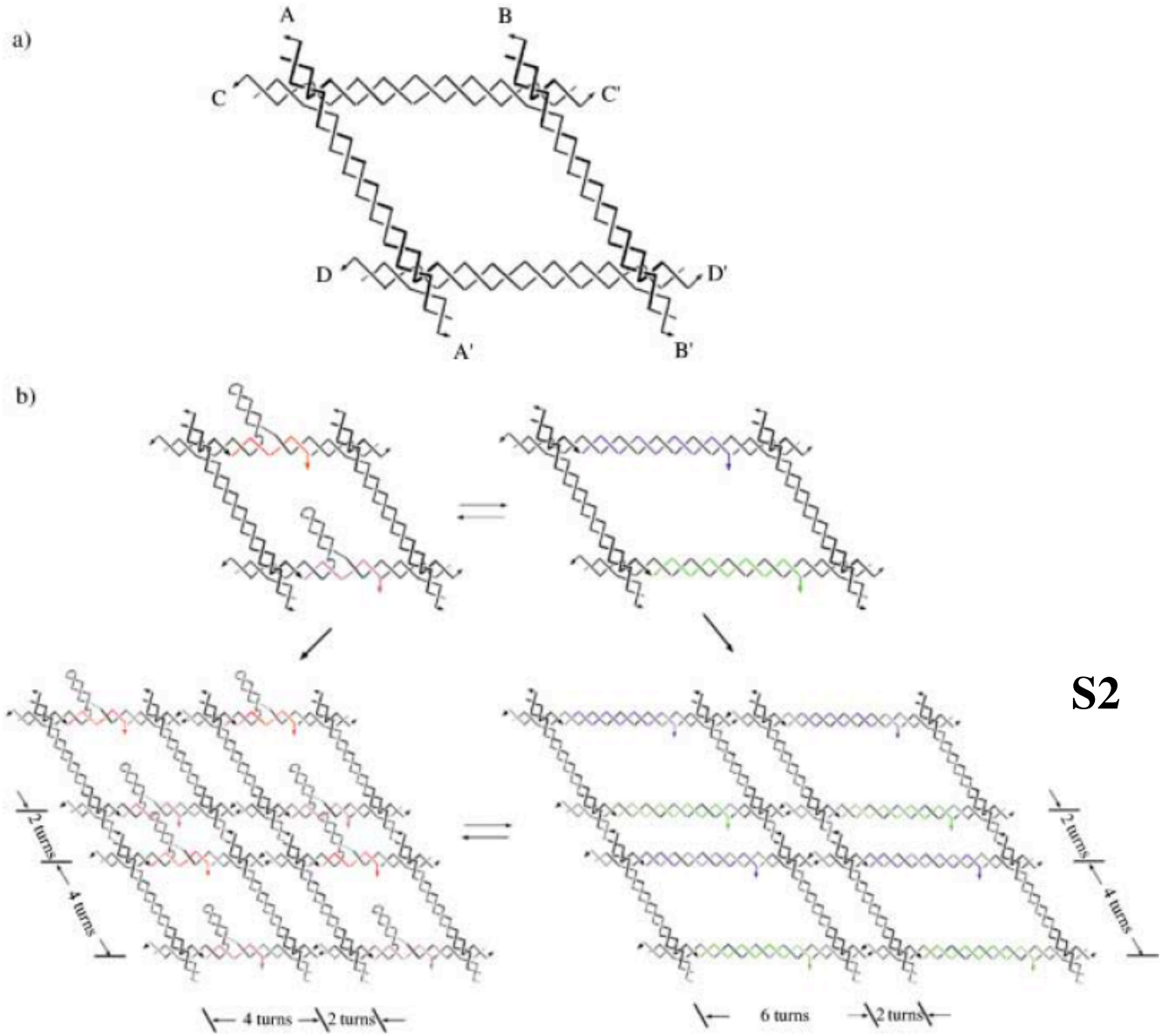

Angew. Chem. Int. Ed. 2003, 42, 4342–4346

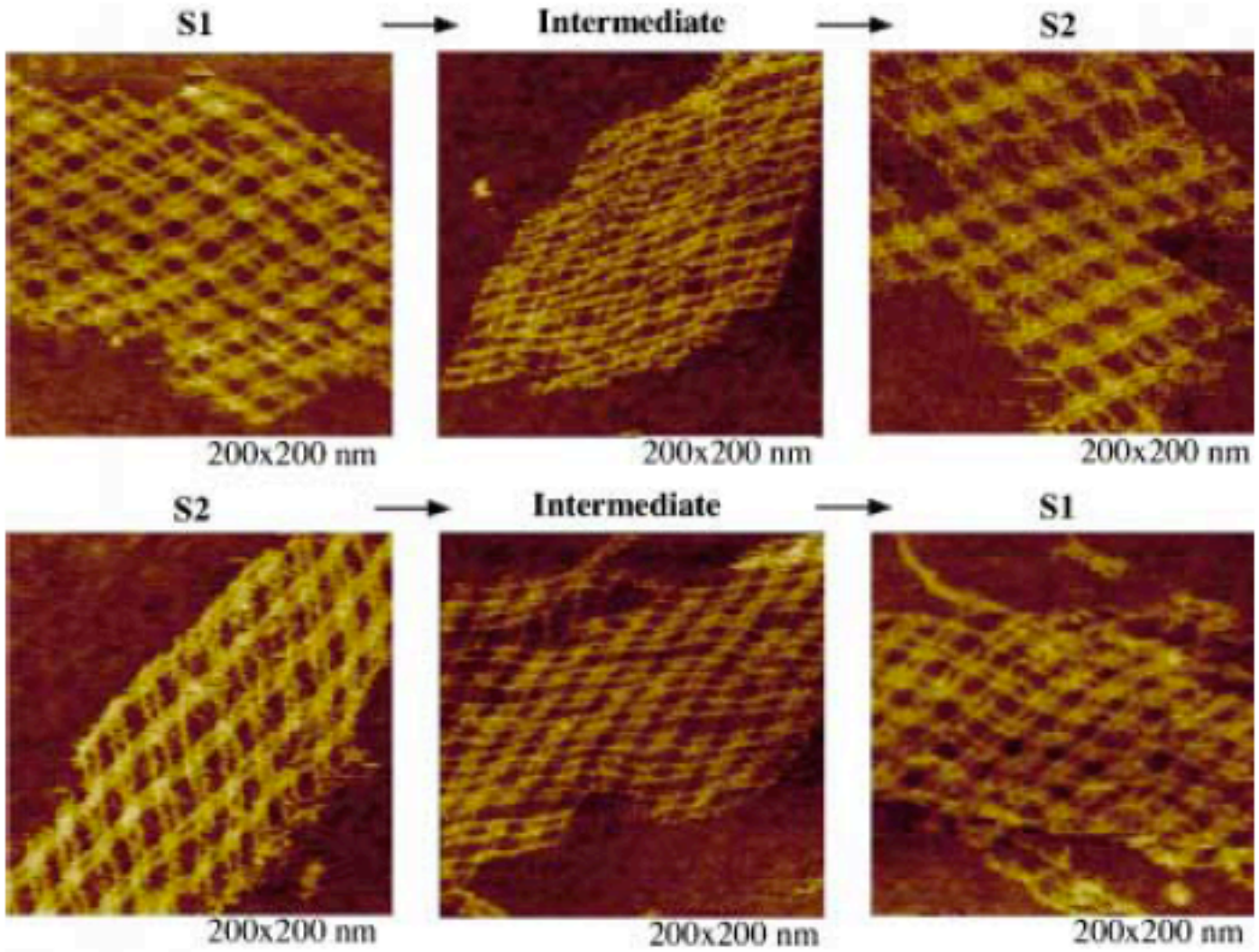

Figure 5. AFM evidence for the two state DNA lattice actuated by DNA nanoactuator devices. For details see text.

A Precisely Controlled DNA Biped Walking Device

William B. Sherman and Nadrian C. Seeman*

NANO LETTERS
2004
Vol. 4, No. 7
1203–1207

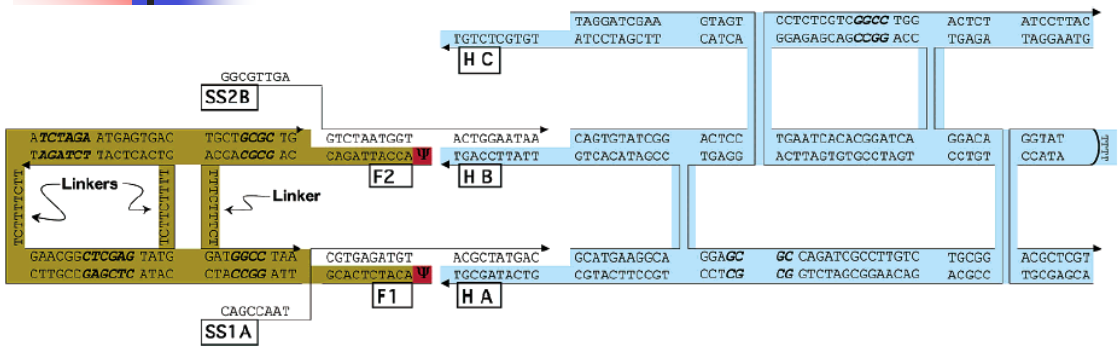

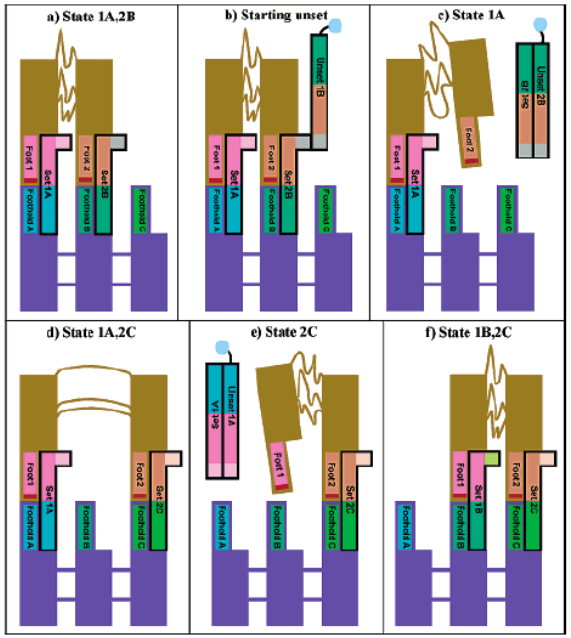

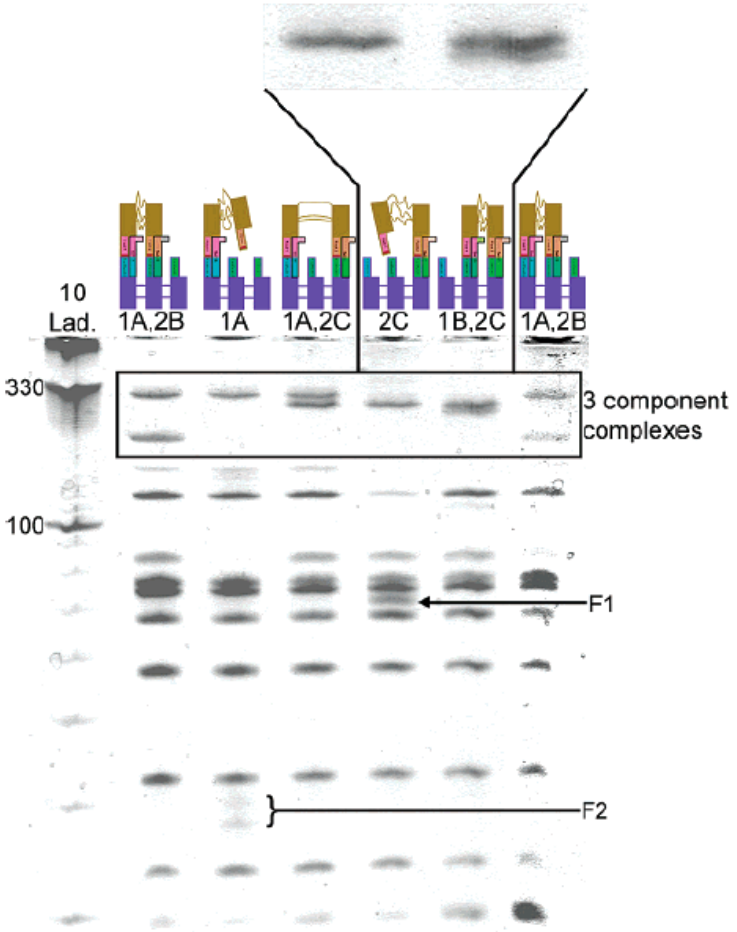

A Unidirectional DNA Walker That Moves Autonomously along a Track**

Angew. Chem. Int. Ed. 2004, 43, 4906–4911

Peng Yin, Hao Yan, Xiaoju G. Daniell, Andrew J. Turberfield,* and John H. Reif**

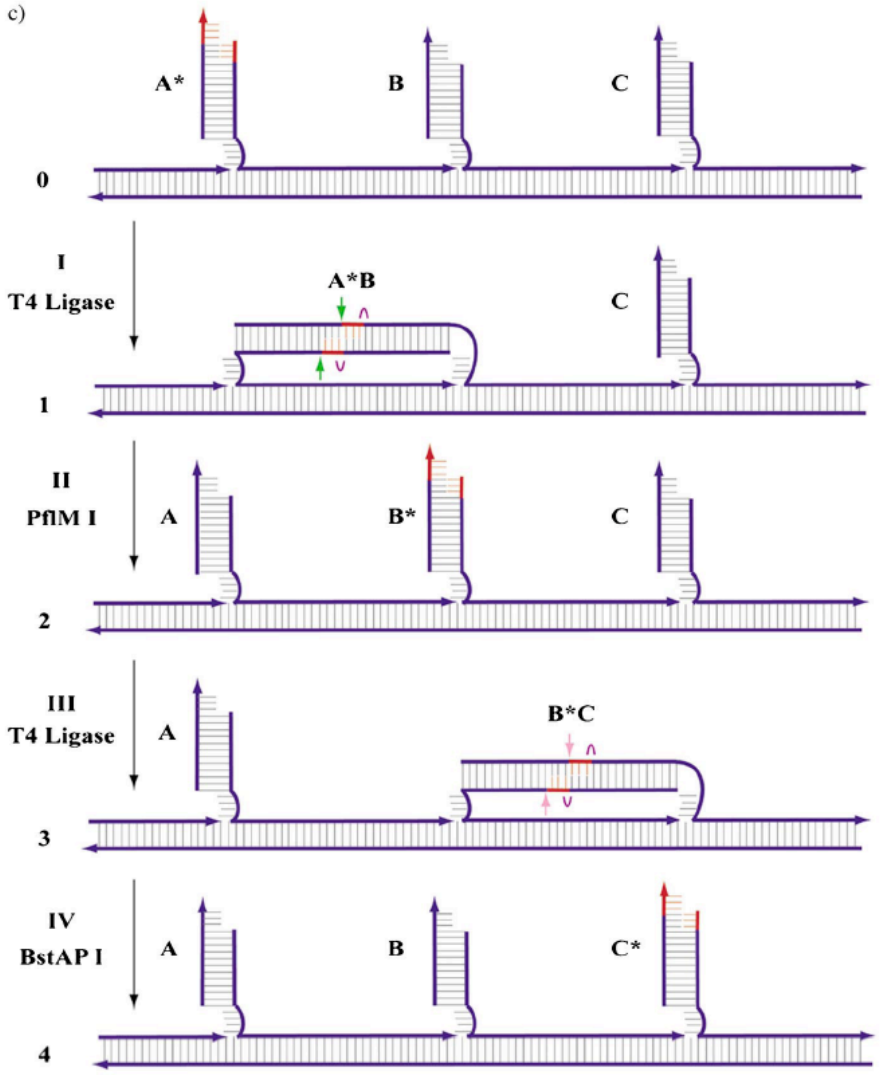

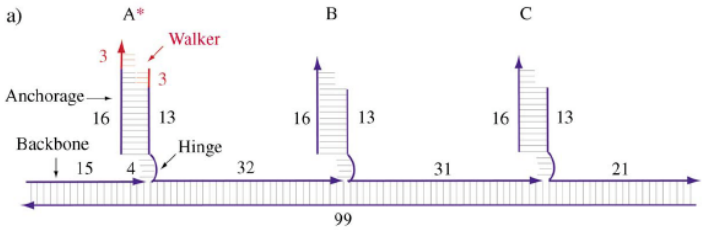

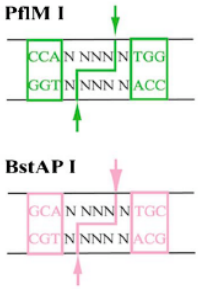

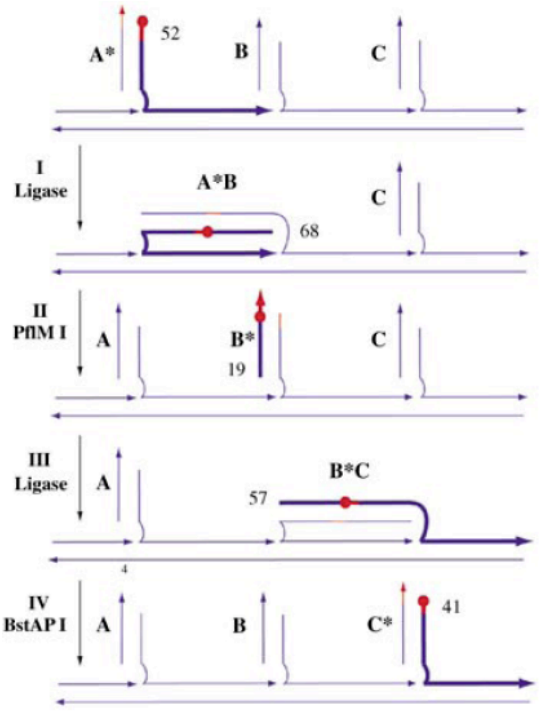

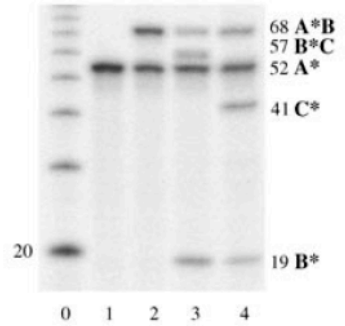

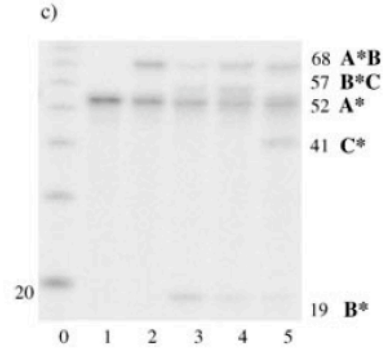

Molecular Gears: A Pair of DNA Circles Continuously Rolls against Each Other

Ye Tian and Chengde Mao* J. AM. CHEM. SOC. 2004, *126*, 11410–11411

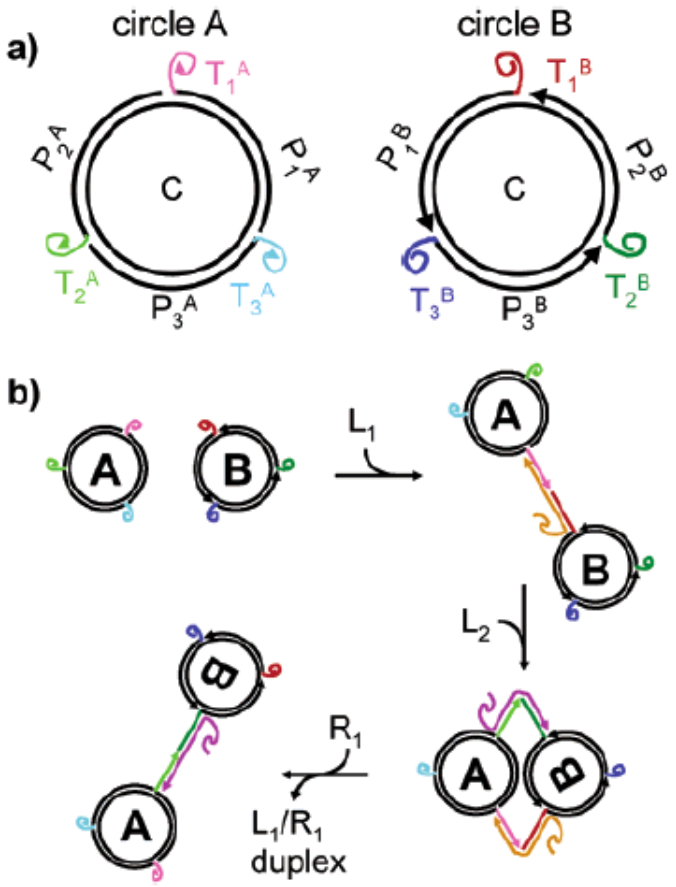

Figure 1. Scheme of the rolling process of gears. (a) Structures of the individual gears. C and P indicate DNA strands, and T indicates teeth. (b) Operation of the gears. L and R represent linker and removal strands, respectively. L_1 and R_1 are complementary to each other. Both circles remain intact during the rolling process. The only changed strands are the linker (L) and removal (R) strands. Note that no twisting motion will be generated to the central stands during the rolling process.

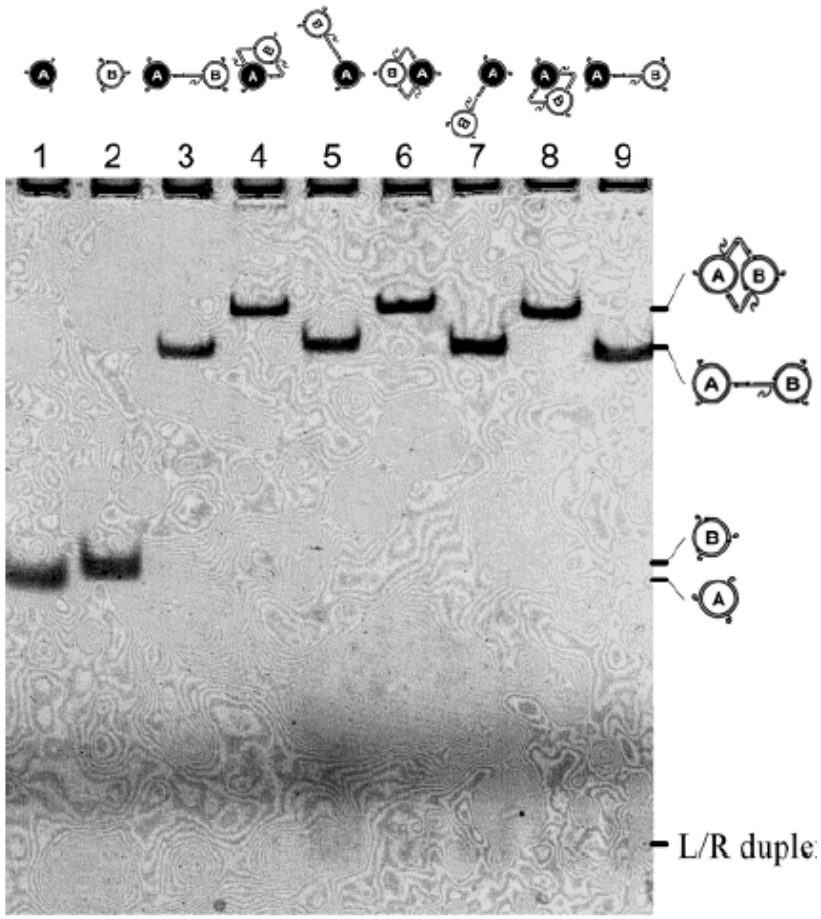

Figure 3. Native PAGE (6%) analysis of the gear rolling process.

A DNAzyme That Walks Processively and Autonomously along a One-Dimensional Track**

*Ye Tian, Yu He, Yi Chen, Peng Yin, and Chengde Mao**

Angew. Chem. Int. Ed. 2005, 44, 4355–4358

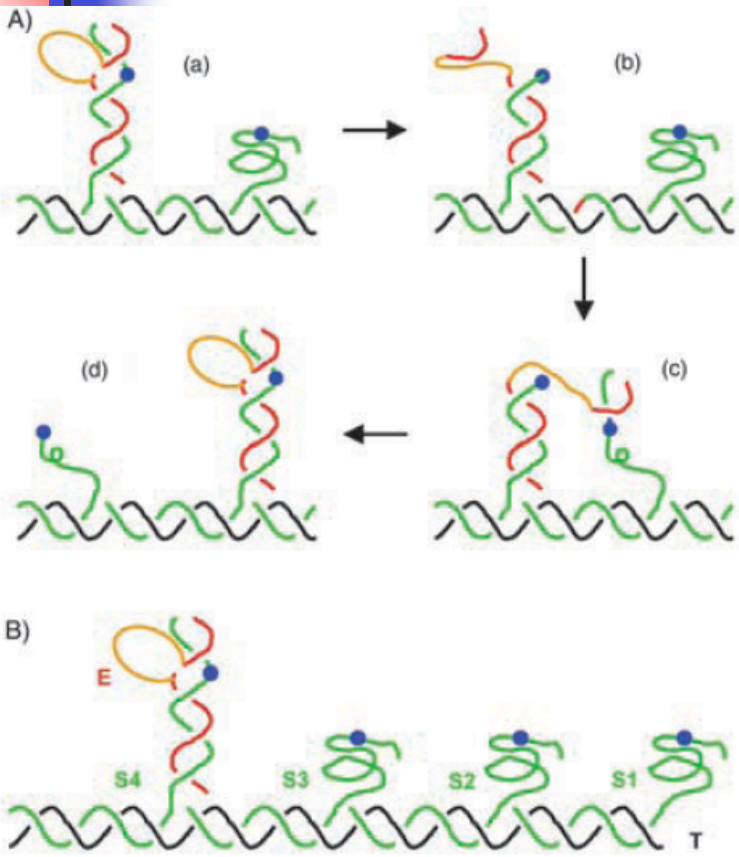

Figure 1. Scheme of a walking DNAzyme and its track. A) The walking principle. B) A construction where the walking DNAzyme is at one end of its track. Black lines: template (**T**); green lines: substrate (**S**); red/yellow lines: a 10–23 DNAzyme (red), with the catalytic core highlighted (yellow); blue dots indicate the bonds to be cleaved by the DNAzyme.

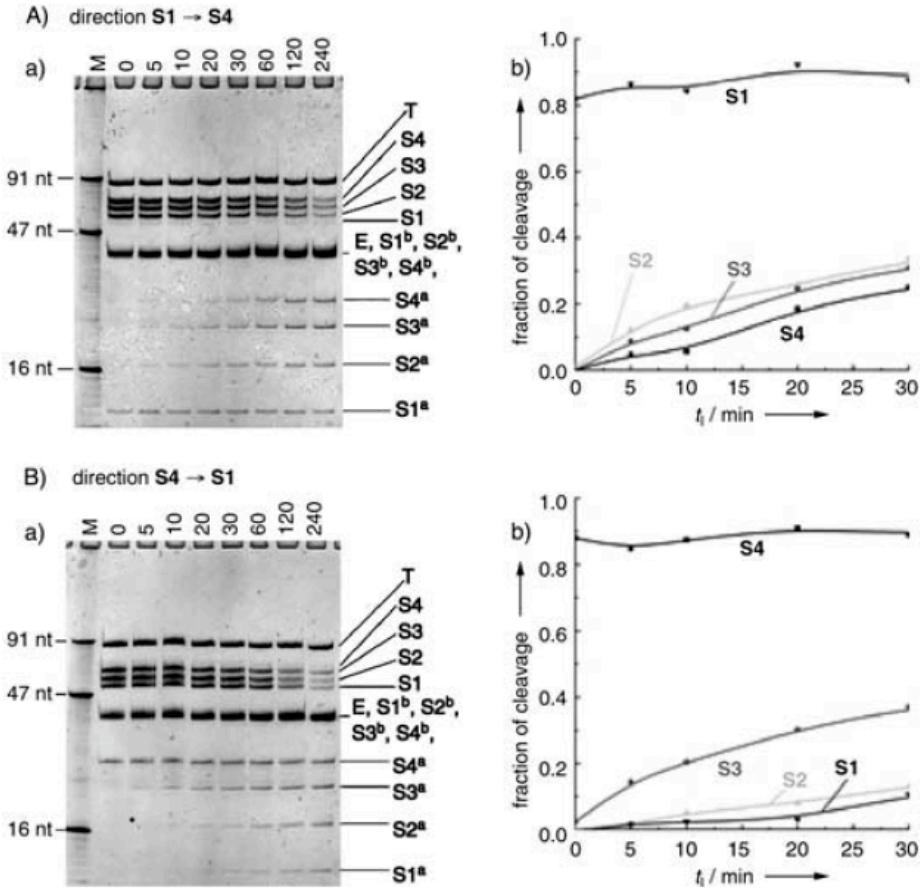

Figure 3. Denaturing PAGE monitoring the movement of the DNAzyme at 22 °C in the directions **S1**→**S4** (A) and **S4**→**S1** (B): a) gel images as a function of incubation time, t_1 (lanes M contain three single-stranded DNA size markers; nt = nucleotide (bases); superscripts a and b denote short and long cleaved substrate fragments, respectively); b) quantification of the differential substrate cleavage.